Remaining Useful Life Prediction of Individual Units Subject to Hard Failure

QIANG ZHOU[1*], JUNBO SON[2], SHIYU ZHOU[2], XIAOFENG MAO[3], MUTASIM SALMAN[3]

[1] *Department of Systems Engineering and Engineering Management, City University of Hong Kong, Kowloon, Hong Kong*
E-mail: q.zhou@cityu.edu.hk
[2] *Department of Industrial and Systems Engineering, University of Wisconsin-Madison, WI 53706, USA*
[3] *General Motors Research & Development, Warren, MI, USA*

Abstract

To develop a cost-effective condition-based maintenance strategy, accurate prediction of remaining useful life (RUL) is the key. It is known that many failure mechanisms in engineering can be traced back to some underlying degradation processes. In this paper, we propose a two-stage prognostic framework for individual units subject to hard failure, based on joint modeling of degradation signal and time-to-event data. The proposed algorithm features low computational load, online prediction and dynamic updating. Its application to automotive battery RUL prediction has been discussed in this paper as an example. The effectiveness of the proposed method has been demonstrated through both simulation study and real data.

Keywords: Remaining useful life prediction, hard failure, joint model

1. Introduction

In engineering applications, the reliability of a critical unit is crucial to guarantee the overall functional capabilities of the entire system. Failure of such a unit can be catastrophic. Turbine engines of airplanes, power supplies of computers, and batteries of automobiles are typical examples where failure of the unit would lead to breakdown of the entire system. For these reasons, such critical units must be well-maintained for the overall system reliability and to improve end user satisfaction. In traditional maintenance strategies, unit is either repaired after its failure (run-to-failure maintenance) or scheduled for time-based preventive maintenance (planned maintenance). In recent years, a more cost-effective

* Corresponding author

strategy called condition-based-maintenance (CBM) (Jardine, Lin, and Banjevic (2006); Ye, Shen, and Xie (2012)) has been proposed. The rationale supporting this procedure is that many system failure mechanisms can be traced back to some underlying degradation processes. RUL prediction can be made based on degradation signal collected. The degradation signal should be strongly associated with the failure of the unit and contains important information about its health status. As the prediction is preferably to be made online for units working in the field, a prognostic algorithm featuring real-time prediction with a low computational requirement is desirable.

With the availability of degradation signal, RUL distribution is typically estimated based on modeling the degradation signal hitting some pre-determined failure threshold (e.g., Lu and Meeker (1993); Gorjian *et al.* (2009); Gebraeel (2006); Ye and Chen (2014)). These methods are called first-hitting-time (FHT) models and the failure they are dealing with is called *soft failure*. However, *hard failure*, where the unit keeps working until it breaks down, is also quite common in practice. The key difference is that the degradation signals will normally exhibit different values at failure. In some applications, it is also possible that a fixed failure threshold is hard to specify due to the following reasons: (1) the threshold depends on the unit's individual specific characteristics, which varies randomly from unit to unit due to variation in their manufacturing process; (2) there are multiple potential failure mechanisms contributing to the same degradation signal; (3) the failure threshold for the degradation signal is a 'gray' area. Non-existence of a fixed failure threshold poses significant difficulties to FHT algorithms. Very limited literature can be found in the engineering field dealing with the prognosis under hard failure (Liao *et al.* (2006); Wang and Coit (2007); Yu and Fuh (2010)). On the other hand, time-to-event data about the failure or censoring information may also be available besides degradation signal in many applications. Time-to-event data contain useful information about life time distribution and has been extensively used in traditional reliability engineering. In engineering field, however, these two types of data are rarely analyzed together in an integrated fashion to extract the full information contained within both.

The integrated analysis of the degradation data and time-to-event data makes possible the prognosis without a fixed failure threshold. Joint modeling of time-to-event data and degradation signal has been

studied in the area of clinical trials, where it is common to collect time-to-event outcome together with some repeated measurements of patients during the study. Comprehensive reviews of the related methods in joint modeling can be found in Yu *et al.* (2004), and Tsiatis and Davidian (2004). The measurement, often called 'surrogate marker' or 'biomarker' in the related literature, is strongly associated with the death of the patient or recurrence of some disease and hence acts as a critical health indicator. Two mostly well-known examples in the clinical study are CD4 lymphocyte count in AIDS (Tsiatis *et al.* (1995); Bycott and taylor (1998); Wang and Taylor (2001)) and PSA level for early detection and recurrence of prostate cancer (Pauler and Finkelstein (2002); Yu, Taylor, and Sandler (2008); Yu *et al.* (2004)). Under the joint modeling framework, degradation signal is often modeled by mixed effects model (Laird and Ware (1982)) and time-to-event data are modeled by the Cox proportional hazard (PH) model (Cox (1972)). The surrogate marker is used as a time-dependent covariate in the Cox PH model so that changes of the surrogate marker impacts the hazard rate. In this approach, the failure of a unit does not depend on a specific threshold but is rather described probabilistically by the hazard function in the Cox PH model. These unique advantages make it a suitable tool for RUL prediction in engineering applications previously described. However, joint modeling in biostatistics has been predominantly focused on studying the impact of covariates on the hazard rate of the population. Very few attempts have been made to study its application in prognosis, particularly RUL prediction for individuals (Pauler and Finkelstein (2002); Yu, Taylor, and Sandler (2008); Rizopoulos (2011)). Furthermore, the joint modeling framework is computationally intensive, posing significant difficulties to its implementation in real-time online prediction for engineering applications.

The joint model is an extension of the Cox PH model with an additional model for the degradation signal. The model allows unit-to-unit variations of the degradation path by using the mixed effects model. Traditionally, degradation signal can be simply incorporated into a Cox PH model as a time-dependent covariate, but with notable difficulties in parameter estimation if observed signals are used directly (Yu *et al.* (2004)). Cox PH model treats the observation as deterministic without random error, hence parameters estimation is biased towards null and the amount of bias is proportional to the magnitude of the random

error in the degradation signal (Prentice (1982)).

In this paper, we propose a prognostic framework for individual unit RUL prediction under hard failure, based on the idea of joint modeling of the time-to-event data and degradation signal. In this method, we assume historical records of a group of similar units are available for model fitting and degradation signal of the unit to be predicted can be obtained. A two-stage approach, containing an offline modeling stage based on the database and an online prediction stage based on the individual unit's degradation signal, has been proposed. The proposed model allows continuous updating of the failure distribution based on the observed signal from the in-service unit. The model updating can be done by a closed-form Bayesian formula, thus the computational burden can be significantly reduced. The method's low computation at the online stage makes it possible to be implemented in the field. For example, automotive engineers are interested in the online prediction of automotive battery RUL, which impacts customer satisfaction and warranty cost to the company. A vital health indicator of the automotive battery is its internal resistance which can be estimated based on engine cranking signal through an ohmic relationship (Zhang *et al.* (2011)) or through more complicated algorithms such as the fractional order model discussed by Cugnet *et al.* (2010). The proposed prognostic algorithm has a low requirement on computation so that it has the potential to be implemented in vehicle onboard micro-controllers.

The rest of this paper is organized as follows. The problem formulation and a detailed description of the proposed method are given in Section II. Section III presents a simulation study where the effectiveness of the proposed method is demonstrated. Section IV applies the method to real data from a battery aging test. Finally, Section V concludes the paper and discusses some possible future work.

2. Prediction on RUL

2.1. *The prognostic framework*

The proposed prognostic framework is composed of two stages: the offline modeling stage, and the online prediction stage. During the offline stage, parameters of the prognostic model are estimated based on a historical database that contains event times, time-stamped degradation signal and possibly some other time-fixed covariates (such as manufacturer, device type, etc.) for a number of similar units. During

the online stage, degradation signal of an in-service unit is obtained and used for prediction of the unit's RUL based on the model parameters estimated during the offline stage. The predictions made for an in-service unit can be updated as more measurements on the degradation signal are obtained during its usage.

Regarding the computational load for the algorithm, there is no stringent requirement for the offline stage as it only has to run once to estimate the population parameters when building the prognostic model, or once in a while when data collected from additional units are added to the database and updated parameter estimates are desired. However, it is desirable to keep the computational load at a low level for the online stage.

2.2. ***Modeling***

Assume the database contains historical data of N similar units, which can be viewed as a random sample from the same underlying population. For the ith unit, its associated data is denoted as $D_i = \{V_i, \delta_i, \boldsymbol{r}_i^h, \boldsymbol{w}_i\}$, where $V_i = \min(T_i, C_i)$ is the event time (the unit either failed at time T_i or was censored at time C_i without knowing its actual time of failure), δ_i is an event indicator corresponds to the type of the event (δ_i = 1/0 indicates the unit has failed/censored), $\boldsymbol{r}_i^h = \{r_{i1}, r_{i2}, ..., r_{in_i}\}^T = \{r_i(t_{i1}), r_i(t_{i2}), ..., r_i(t_{in_i})\}^T$ is the history of observed degradation signal (e.g., internal resistance of a battery) with $t_{in_i} \le V_i$, and the vector $\boldsymbol{w}_i$ contains all the other time-fixed covariates that are associated with the unit. Note that the time components in the dataset are not absolute times measured in calendar date but relative time lengths starting from the moment when the unit came into service. Based on the nature of data $D_i = \{V_i, \delta_i, \boldsymbol{r}_i^h, \boldsymbol{w}_i\}$, the modeling approach involves two distinct sub-modeling approaches: longitudinal analysis for the degradation signal and survival analysis for the time-to-event data.

2.2.1. Sub-model I: Longitudinal analysis for the degradation signal

In this section, the degradation path of the signal will be modeled through random effects model, by assuming the degradation process follows some parametric path. Degradation signal provides important

information as the health status of a unit and hence modeling of its evolution will facilitate the prognosis of its RUL. The random coefficients in the model are particularly suitable for describing the variations among a population of similar units.

Without loss of generality, we assume the degradation signal increases as the unit degrades (e.g., a battery's resistance increases as it ages). The degradation path of the *i*th unit is assumed to follow the model:

$$r_i(t) = x_i(t) + \varepsilon_i(t) = \boldsymbol{z}^T(t)\boldsymbol{b}_i + \varepsilon_i(t) \ , \tag{1}$$

where $x_i(t)$ is the true but unobservable value of the degradation signal, $\varepsilon_i(t)$ is the measurement error which is assumed to be independent and follows normal distribution $N(0, \sigma^2)$, $\boldsymbol{z}^T(t)$ contains the intercept and time-dependent regression functions and $\boldsymbol{b}_i$ is a vector of random coefficients. With the random coefficients, model (1) assumes those units have distinct but similar degradation paths.

In cases where nonlinear behaviors of degradation signal are evident, we may add higher order polynomial terms or splines in $\boldsymbol{z}^T(t)$. We may also include certain specific nonlinear functions of time (e.g., log(*t*) or $t^{0.5}$) in the model, if they are believed to be the correct forms based on either physical knowledge or empirical results. However, identifying a single best growth model that works for all applications is impossible and hard to justify. $\boldsymbol{z}^T(t)$ is a user-defined function requiring domain knowledge and experience of the specific system degradation process. It should be defined on a case by case basis. Figure 1 shows an example of resistance measurements of 10 lead acid batteries during an accelerated aging test on their engine cranking capability. From the motivating data and the dataset illustrated in Figure 7, we have found that the quadratic form would be appropriate to describe the degradation signal propagation for the particular application of automotive lead-acid batteries. The quadratic structure or polynomial in general, has been commonly used in the prognosis literature for individual components (Gebraeel (2006); Gebraeel *et al.* (2005); Elwany, A. *et al.* (2009)). The polynomial model can also be transformed to handle the exponential or the power form (Gebraeel *et al.*

(2005)).

For the random effects, we assume $\boldsymbol{b}_i$ follows a multivariate normal distribution $N(\boldsymbol{\mu}_b, \boldsymbol{\Sigma}_b)$, possibly after some transformation of the signal. Studies conducted by Rizopoulos and Verbeke (2008), and Hsieh, Tseng, and Wang (2006) show the model parameter estimates are rather robust to misspecification of the random effects distribution, particularly as the number of measurements per unit increases. Note that the time points when measurements are made may be different for various units: for the *i*th unit, its degradation signal was measured at times: $t_{i1}, t_{i2}, \ldots, t_{in_i}$.

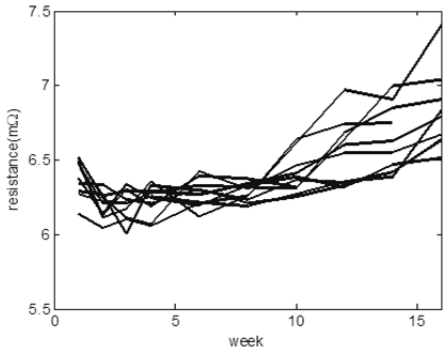

Figure 1. Resistances of 10 lead acid batteries during an accelerated aging test

2.2.2. Sub-model II: Survival analysis for time-to-event data

In this section, we model the time-to-event data (V_i, δ_i) based on time-fixed covariates $\boldsymbol{w}_i$ and time-dependent covariates $x_i(t)$ from the degradation model previously described. Typically, $x_i(t)$ would be associated with a single coefficient to reflect its impact on the hazard rate. For greater flexibility, we split $x_i(t)$ into two components, its initial value $x_i(0)$ and its increase $x_i(t) - x_i(0)$, and associate them with two different coefficients. This allows the two components to have different impacts on the hazard rate, a phenomenon we have observed in the application of automotive batteries. By expressing $\boldsymbol{z}^T(t) = [1, \boldsymbol{z}_1^T(t)]$ and $\boldsymbol{b}_i = [b_{i0}, \boldsymbol{b}_{i1}^T]^T$, we have assumed the following form for hazard rate of the *i*th unit:

$$h_i(t) = h_0(t) \exp[\boldsymbol{\gamma}^T \boldsymbol{w}_i + \beta_0 b_{i0} + \beta_1 \boldsymbol{z}_1^T(t) \boldsymbol{b}_{i1}], \tag{2}$$

where $h_0(t)$ is the baseline hazard rate, $\boldsymbol{\gamma}$ is a vector of association parameters linking fixed covariate(s)

in $\boldsymbol{w}_i$ with the hazard rate, β_0 and β_1 are the parameters linking the degradation signal initial value and its increase with the hazard rate, respectively. If imposing the constraint $\beta_0 = \beta_1$, (2) will reduce to the typical formulation where the entire degradation signal $x_i(t)$ is associated with a single parameter β. Basically, the degradation signal is included as a factor for the hazard rate function. Factors that impact the lifetime of units manifest themselves through the degradation signal. Thus, the degradation signal value gives us a good idea of the unobservable health status of the unit.

Note $h_0(t)$, $\boldsymbol{\gamma}$, β_0 and β_1 do not depend on i; they represent population characteristics while individual specific information is contained in $\boldsymbol{w}_i$ and $\boldsymbol{b}_i$. The baseline hazard rate $h_0(t)$ can be assumed to have some parametric forms such as Weibull, or some step function, but can also be nonparametric for better flexibility. The two sub-models, (1) and (2), share the same random effects $\boldsymbol{b}_i$ and are conditionally independent given $\boldsymbol{b}_i$. We use $\boldsymbol{\Theta} = \{\boldsymbol{\mu}_b, \boldsymbol{\Sigma}_b, \boldsymbol{\gamma}, \beta_0, \beta_1, \sigma^2\}$ to collectively denote all the parameters in the two models.

It is worth pointing out the difference between the conventional Cox PH model and the joint model in terms of prognosis. One simple extension from the Cox PH model would be having a simple regression model for the degradation signal to predict its future value, e.g., $\boldsymbol{z}^T(t)\boldsymbol{b}$. However, this would produce the same prediction results for all future units (with the same $\boldsymbol{w}_i$). The joint model uses mixed effects model to account for unit-to-unit variations by allowing $\boldsymbol{b}$ to be random, providing individualized prediction results for each in-service unit.

2.3. *Parameter estimation*

In practice, $\boldsymbol{\Theta}$ and $h_0(t)$ are unknown and need to be estimated based on the database information. Based on the conditional independence, the observed data likelihood for the ith unit in the database is (note $\boldsymbol{b}_i$ is unobservable)

$$\begin{aligned} p(V_i, \delta_i, \boldsymbol{r}_i^h, \boldsymbol{w}_i; \boldsymbol{\Theta}) &= \int p(V_i, \delta_i, \boldsymbol{r}_i^h \mid \boldsymbol{w}_i, \boldsymbol{b}_i; \boldsymbol{\Theta}) p(\boldsymbol{b}_i; \boldsymbol{\Theta}) d\boldsymbol{b}_i \\ &= \int p(V_i, \delta_i \mid \boldsymbol{w}_i, \boldsymbol{b}_i; \boldsymbol{\Theta}) p(\boldsymbol{r}_i^h \mid \boldsymbol{b}_i; \boldsymbol{\Theta}) p(\boldsymbol{b}_i; \boldsymbol{\Theta}) d\boldsymbol{b}_i \end{aligned}, \tag{3}$$

where $p(V_i, \delta_i \mid \boldsymbol{w}_i, \boldsymbol{b}_i; \Theta)$ corresponds to the survival model and $p(\boldsymbol{r}_i^h \mid \boldsymbol{b}_i; \Theta)$ corresponds to the degradation model. The three components in Equation (3) are:

$$\begin{aligned} & p(V_i, \delta_i \mid \boldsymbol{w}_i, \boldsymbol{b}_i; \Theta) = [h_i(V_i \mid \boldsymbol{w}_i, \boldsymbol{b}_i; \Theta)]^{\delta_i} S_i(V_i \mid \boldsymbol{w}_i, \boldsymbol{b}_i; \Theta) \\ & = \left[h_0(V_i) \exp[\boldsymbol{\gamma}^T \boldsymbol{w}_i + \beta_0 b_{i0} + \beta_1 \boldsymbol{z}_1^T(V_i) \boldsymbol{b}_{i1}] \right]^{\delta_i} \exp\left\{ -\int_0^{V_i} h_0(u) \exp[\boldsymbol{\gamma}^T \boldsymbol{w}_i + \beta_0 b_{i0} + \beta_1 \boldsymbol{z}_1^T(u) \boldsymbol{b}_{i1}] du \right\} \end{aligned}, \quad (4)$$

$$p(\boldsymbol{r}_i^h \mid \boldsymbol{b}_i; \Theta) = \prod_{j=1}^{n_i} p[r_{ij} \mid \boldsymbol{b}_i; \Theta] = \prod_{j=1}^{n_i} \frac{1}{\sqrt{2\pi\sigma^2}} \exp\left\{ -\frac{1}{2} \frac{[r_{ij} - \boldsymbol{z}^T(t_{ij}) \boldsymbol{b}_i]^2}{\sigma^2} \right\}, \quad (5)$$

and

$$p(\boldsymbol{b}_i; \Theta) = \frac{1}{(2\pi)^{k/2} |\boldsymbol{\Sigma}_b|^{1/2}} \exp\left[-\frac{1}{2} (\boldsymbol{b}_i - \boldsymbol{\mu}_b)^T \boldsymbol{\Sigma}_b^{-1} (\boldsymbol{b}_i - \boldsymbol{\mu}_b) \right], \quad (6)$$

where k is the number of parameters in $\boldsymbol{b}_i$. There are two ways for parameter estimation using the likelihood functions defined in (4), (5) and (6). One is directly maximizing the joint log-likelihood function defined as $\sum_{i=1}^{N} \log\left[p(V_i, \delta_i, \boldsymbol{r}_i^h, \boldsymbol{w}_i; \Theta) \right]$ and the other employs the EM algorithm by treating $\boldsymbol{b}_i$ as missing variable (Wulfsohn, M., and Tsiatis, A. (1997)). The joint likelihood function has a complex form, making both methods computationally demanding. To alleviate the computational load, a "two-stage" approximation method has been used frequently in the joint modeling literature (Tsiatis, Degruttola and Wulfsohn (1995)). It estimates the parameters in the mixed effects model first, then estimates the parameters in the Cox PH model by treating the mixed effects model as known. In this way, the mixed effects model provide "true" values of the time-dependent covariate at any time point to facilitate the estimation of the Cox PH model. Doing so will introduce some bias (Tsiatis, Degruttola and Wulfsohn (1995); Bycott and Taylor (1998)). Fortunately, according to a comparison study between the EM algorithm and the two-stage method, the difference is negligible (Wulfsohn and Tsiatis (1997)). For this reason, the two-stage method is well-accepted in literature for its efficient computation with negligible bias (Yu *et al.* (2004)). In the following sections, we let $\hat{\Theta}$ and $\hat{h}_0(t)$ denote the estimated parameters.

2.4. *Predicting the RUL of a new unit*

Based on the model previously described and its estimated parameters, predictions can be made for the RUL of a new in-service unit p during the online stage. This new unit is similar to those contained in the database, and they can be considered as individuals sampled from the same population. We assume that unit p is still in use and its degradation signal is obtained intermittently during its usage. As individual specific information is contained within $\boldsymbol{w}_p$ and $\boldsymbol{b}_p$ (i.e., the time independent covariate and degradation path coefficient of unit p), we need to estimate $\boldsymbol{b}_p$ based on its degradation signal in order to make the prediction ($\boldsymbol{w}_p$ is normally known in practice). We use a Bayesian update scheme, where both the population information contained in the database and the individual specific information contained in its degradation signal can be blended together for estimation.

2.4.1. Bayesian estimation for unit p

At the time instant t^* when the prediction is to be made, assume there are m values of degradation signal available for unit p: $\boldsymbol{r}_p^* = \{r_{p1}, r_{p2}, ..., r_{pm}\}^T = \{r_p(t_{p1}), r_p(t_{p2}), ..., r_p(t_{pm})\}^T$, where $t_{pm} \le t^*$. The degradation model for unit p is:

$$r_p(t) = x_p(t) + \varepsilon_p(t) = \boldsymbol{z}^T(t)\boldsymbol{b}_p + \varepsilon_p(t).$$

For convenience, we write the above equation in the following matrix form

$$\boldsymbol{r}_p^* = \boldsymbol{Z}_p^* \boldsymbol{b}_p + \boldsymbol{E}_p^*,$$

where $\boldsymbol{E}_p^* = [\varepsilon_p(t_{p1}), \varepsilon_p(t_{p2}), ..., \varepsilon_p(t_{pm})]^T$ is the $m \times 1$ error vector, and $\boldsymbol{Z}_p^*$ is an $m \times k$ matrix given as below

$$\boldsymbol{Z}_p^* = \begin{bmatrix} \boldsymbol{z}^T(t_{p1}) \\ \boldsymbol{z}^T(t_{p2}) \\ \cdots \\ \boldsymbol{z}^T(t_{pm}) \end{bmatrix}.$$

The asterisk indicates the variables are dependent upon the time instant t^*.

Specification of a prior in a Bayesian approach typically depends on the availability of closely related

historical data and/or expert knowledge. In our case, it is natural to choose the prior based on the database information as we consider the unit p and the database units are similar. Using the estimated distribution of $\boldsymbol{b}_i$ as the prior for $\boldsymbol{b}_p$, the posterior distribution of $\boldsymbol{b}_p$ is

$$p(\boldsymbol{b}_p \mid \boldsymbol{r}_p^*) \propto p(\boldsymbol{r}_p^* \mid \boldsymbol{b}_p)\pi(\boldsymbol{b}_p),$$

where $\pi(\boldsymbol{b}_p) = N(\hat{\boldsymbol{\mu}}_b, \hat{\boldsymbol{\Sigma}}_b)$ is the prior distribution of $\boldsymbol{b}_p$ and $p(\boldsymbol{r}_p^* \mid \boldsymbol{b}_p)$ is the likelihood function given as

$$p(\boldsymbol{r}_p^* \mid \boldsymbol{b}_p) = \prod_{j=1}^{m} p[r_{pj} \mid \boldsymbol{b}_p; \hat{\boldsymbol{\Theta}}] = \prod_{j=1}^{m} \frac{1}{\sqrt{2\pi\hat{\sigma}^2}} \exp\left\{-\frac{1}{2}\frac{[r_{pj} - \boldsymbol{z}^T(t_{pj})\boldsymbol{b}_p]^2}{\hat{\sigma}^2}\right\}. \quad (7)$$

It can be shown through straightforward derivation that the posterior distribution is also multivariate normal. Assume $p(\boldsymbol{b}_p \mid \boldsymbol{r}_p^*) = N(\hat{\boldsymbol{\mu}}_p^*, \hat{\boldsymbol{\Sigma}}_p^*)$, we have

$$\begin{cases} \hat{\boldsymbol{\mu}}_p^* = \hat{\boldsymbol{\Sigma}}_p^*\left[(\boldsymbol{Z}_p^*)^T \boldsymbol{r}_p^* / \hat{\sigma}^2 + (\hat{\boldsymbol{\Sigma}}_b)^{-1}\hat{\boldsymbol{\mu}}_b\right] \\ \hat{\boldsymbol{\Sigma}}_p^* = \left[(\hat{\boldsymbol{\Sigma}}_b)^{-1} + (\boldsymbol{Z}_p^*)^T \boldsymbol{Z}_p^* / \hat{\sigma}^2\right]^{-1} \end{cases}.$$

Proof of the above result is given in the Appendix. This neat closed form update for the distribution of $\boldsymbol{b}_p$ allows the parameter estimation to be made with a low computation effort during online stage. Since we use the two-stage estimation scheme, the $p(\boldsymbol{b}_p \mid \boldsymbol{r}_p^*)$ can be re-estimated, or updated, without considering the $p(V_i, \delta_i \mid \boldsymbol{w}_i, \boldsymbol{b}_i; \boldsymbol{\Theta})$. Thus, the overall computation for the online stage can be reduced significantly.

2.4.2. RUL prediction

Based on the previously estimated parameters, the RUL distribution of unit p can be made in the form of its survival function conditional upon the fact that the unit survives no shorter than t^*. Given $\boldsymbol{b}_p$, the survival function is

$$\begin{aligned} & S(t \mid t^*, \boldsymbol{w}_p, \boldsymbol{b}_p; \hat{\boldsymbol{\Theta}}, \hat{h}_0(t)) \\ &= \frac{S(t \mid \boldsymbol{w}_p, \boldsymbol{b}_p; \hat{\boldsymbol{\Theta}}, \hat{h}_0(t))}{S(t^* \mid \boldsymbol{w}_p, \boldsymbol{b}_p; \hat{\boldsymbol{\Theta}}, \hat{h}_0(t))} \\ &= \exp\{-\int_{t^*}^{t} \hat{h}_0(u) \exp[\hat{\boldsymbol{\gamma}}^T \boldsymbol{w}_p + \hat{\beta}_0 b_{p0} + \hat{\beta}_1 \boldsymbol{z}_1^T(u)\boldsymbol{b}_{p1}]du\} \end{aligned}, \quad (8)$$

where $t \geq t^*$ and the function equals to 1 if $t = t^*$. Based on Equation (8) and the posterior distribution of $\boldsymbol{b}_p$, the estimated survival function can be expressed in the form of a distribution and hence its corresponding point-wise Bayesian credible interval.

In many cases, a point estimate of the survival function may be desirable in practice. Based on Equation (8), the marginal survival function obtained by integrating out $\boldsymbol{b}_p$ is

$$S(t \mid t^*, \boldsymbol{w}_p, \boldsymbol{r}_p^*; \hat{\boldsymbol{\Theta}}, \hat{h}_0(t)) = \int S(t \mid t^*, \boldsymbol{w}_p, \boldsymbol{b}_p; \hat{\boldsymbol{\Theta}}, \hat{h}_0(t)) p(\boldsymbol{b}_p \mid \boldsymbol{r}_p^*) d\boldsymbol{b}_p \,. \tag{9}$$

A special case for Equations (8) and (9) is when $t^* = 0$, i.e., a newly installed unit without any degradation signal available. In such case, we can use the prior distribution $\pi(\boldsymbol{b}_p)$ instead of its posterior distribution to make the prediction. As there is no individual specific information about the unit's degradation path, the prediction will only reflect the population average behavior extracted from the database, adjusted for the time fixed covariate $\boldsymbol{w}_p$.

The evaluation of Equation (9) is computationally demanding due to the multiple integral which has no closed form expression. Because $p(\boldsymbol{b}_p \mid \boldsymbol{r}_p^*)$ is a multivariate normal density function, this integral can be approximated efficiently by using Gauss-Hermite quadrature.

First, we convert $p(\boldsymbol{b}_p \mid \boldsymbol{r}_p^*)$ to a standard multivariate normal distribution of the same dimension by letting $\boldsymbol{b}_p = \hat{\boldsymbol{\mu}}_p^* + A_p^* \boldsymbol{z}$, where A_p^* is a $k \times k$ square matrix from the decomposition $\hat{\boldsymbol{\Sigma}}_p^* = A_p^* \left(A_p^*\right)^T$ and $\boldsymbol{z}$ follows a k-dimensional multivariate standard normal distribution. The existence of A_p^* is guaranteed by the fact that $\hat{\boldsymbol{\Sigma}}_p^*$ is symmetric and positive definite. Define a $k \times 1$ vector $\hat{\boldsymbol{\beta}}_z = \left[\, \hat{\beta}_0 \quad \hat{\beta}_1 \boldsymbol{z}_1^T(t) \,\right]^T$, we have

$$\hat{\beta}_0 b_{p0} + \hat{\beta}_1 \boldsymbol{z}_1^T(t) \boldsymbol{b}_{p1} = \left[\, \hat{\beta}_0 \quad \hat{\beta}_1 \boldsymbol{z}_1^T(t) \,\right] \begin{bmatrix} b_{p0} \\ \boldsymbol{b}_{p1} \end{bmatrix} = \hat{\boldsymbol{\beta}}_z^T \boldsymbol{b}_p = \hat{\boldsymbol{\beta}}_z^T (\hat{\boldsymbol{\mu}}_p^* + A_p^* \boldsymbol{z}) \,. \tag{10}$$

Based on Equations (9) and (10), the change of variable from $\boldsymbol{b}_p$ to $\boldsymbol{z}$ gives us the following result:

$$
\begin{aligned}
&S(t \mid t^*, \boldsymbol{w}_p, \boldsymbol{r}_p^*; \hat{\boldsymbol{\Theta}}, \hat{h}_0(t)) \\
&= \int \exp\{-\int_{t^*}^{t} \hat{h}_0(u) \exp[\hat{\boldsymbol{\gamma}}^T \boldsymbol{w}_p + \hat{\boldsymbol{\beta}}_z^T (\hat{\boldsymbol{\mu}}_p^* + \boldsymbol{A}_p^* \boldsymbol{z})] du\} p(\boldsymbol{z}) d\boldsymbol{z} . \qquad (11) \\
&= \int G(\boldsymbol{z}) p(\boldsymbol{z}) d\boldsymbol{z}
\end{aligned}
$$

where $p(\boldsymbol{z})$ is the probability density function of a k-dimensional standard multivariate normal distribution, and $G(\boldsymbol{z})$ is the remaining part of the integrand. The dependence of $G(\boldsymbol{z})$ on other parameters is suppressed here for simplicity. Based on Equation (11), we have the following approximation for the marginal survival function:

$$
\hat{S}(t \mid t^*, \boldsymbol{w}_p, \boldsymbol{r}_p^*; \hat{\boldsymbol{\Theta}}, \hat{h}_0(t)) = \frac{1}{(2\pi)^{k/2}} \sum_{i_1=1}^{s} \cdots \sum_{i_k=1}^{s} G(z_{1,i_1}, \ldots, z_{k,i_k}) c_{s,i_1} \ldots c_{s,i_k} , \qquad (12)
$$

where s is the number of nodes used, z's are the zeros of sth order Hermite polynomial and c's are their associated weights. Since the survival function is typically smooth and well-behaved as long as N is not too small, we can expect a good approximation with even a small s (e.g., $s < 10$ or even $s < 5$). The evaluation of $G(\boldsymbol{z})$ involves a simple integral over time t, which can be done very fast through either Gauss-Legendre quadrature or any classical numerical integration method such as the Simpson's method. In Equation (12), $G(\boldsymbol{z})$ needs to be evaluated s^k times, which normally is not large since k, the dimension of $\boldsymbol{b}_p$, is usually a small number.

We discuss an alternative estimating method for the marginal survival function that can be evaluated even faster than Equation (12), particularly with large k value. It uses the expected value of the hazard rate function and integrates it over time t. Specifically, since $p(\boldsymbol{b}_p \mid \boldsymbol{r}_p^*)$ is multivariate normal $N(\hat{\boldsymbol{\mu}}_p^*, \hat{\boldsymbol{\Sigma}}_p^*)$, $\hat{\boldsymbol{\gamma}}^T \boldsymbol{w}_p + \hat{\beta}_0 b_{p0} + \hat{\beta}_1 \boldsymbol{z}_1^T(t) \boldsymbol{b}_{p1}$ follows a univariate normal distribution given as

$$
\hat{\boldsymbol{\gamma}}^T \boldsymbol{w}_p + \hat{\beta}_0 b_{p0} + \hat{\beta}_1 \boldsymbol{z}_1^T(t) \boldsymbol{b}_{p1} \sim N(\hat{\boldsymbol{\gamma}}^T \boldsymbol{w}_p + \hat{\boldsymbol{\beta}}_z^T \hat{\boldsymbol{\mu}}_p^*, \hat{\boldsymbol{\beta}}_z^T \hat{\boldsymbol{\Sigma}}_p^* \hat{\boldsymbol{\beta}}_z) .
$$

Hence, $\exp[\hat{\boldsymbol{\gamma}}^T \boldsymbol{w}_p + \hat{\beta}_0 b_{p0} + \hat{\beta}_1 \boldsymbol{z}_1^T(t) \boldsymbol{b}_{p1}]$ follows a lognormal distribution and the expected value of hazard rate function is

$$E[\hat{h}(t)\,|\,\boldsymbol{b}_p] = h_0(t)\exp[\hat{\boldsymbol{\gamma}}^T\boldsymbol{w}_p + \hat{\boldsymbol{\beta}}_z^T\hat{\boldsymbol{\mu}}_p^* + \hat{\boldsymbol{\beta}}_z^T\hat{\boldsymbol{\Sigma}}_p^*\hat{\boldsymbol{\beta}}_z/2]\,.$$

Therefore, we obtain an alternative estimator for the marginal survival function as

$$\widetilde{S}(t\,|\,t^*,\boldsymbol{w}_p,\boldsymbol{r}_p^*;\hat{\boldsymbol{\Theta}},\hat{h}_0(t)) = \exp\{-\int_{t^*}^{t}\hat{h}_0(u)\exp[\hat{\boldsymbol{\gamma}}^T\boldsymbol{w}_p + \hat{\boldsymbol{\beta}}_z^T\hat{\boldsymbol{\mu}}_p^* + \hat{\boldsymbol{\beta}}_z^T\hat{\boldsymbol{\Sigma}}_p^*\hat{\boldsymbol{\beta}}_z/2]du\}\,. \qquad (13)$$

This method is significantly faster than that based on Equation (12) as it primarily involves closed form calculations except the simple integration over time *t*. Another major advantage of this method is that the computational load does not increase much as *k* increases.

It should be pointed out that Equation (13) and Equation (9) are algebraically different. To compare those two methods, let $H(\boldsymbol{b}_p) = -\int_{t^*}^{t}\hat{h}_0(u)\exp[\hat{\boldsymbol{\gamma}}^T\boldsymbol{w}_p + \hat{\beta}_0 b_{p0} + \hat{\beta}_1\boldsymbol{z}_1^T(u)\boldsymbol{b}_{p1}]du$, we can then rewrite Equation (9) as

$$\begin{aligned} S(t\,|\,t^*,\boldsymbol{w}_p,\boldsymbol{r}_p^*;\hat{\boldsymbol{\Theta}},\hat{h}_0(t)) &= \int S(t\,|\,t^*,\boldsymbol{w}_p,\boldsymbol{b}_p;\hat{\boldsymbol{\Theta}},\hat{h}_0(t))\,p(\boldsymbol{b}_p\,|\,\boldsymbol{r}_p^*)d\boldsymbol{b}_p \\ &= \int\exp[H(\boldsymbol{b}_p)]\,p(\boldsymbol{b}_p\,|\,\boldsymbol{r}_p^*)d\boldsymbol{b}_p = E\{\exp[H(\boldsymbol{b}_p)]\} \end{aligned},$$

and Equation (13) as

$$\widetilde{S}(t\,|\,t^*,\boldsymbol{w}_p,\boldsymbol{r}_p^*;\hat{\boldsymbol{\Theta}},\hat{h}_0(t)) = \exp\{E[H(\boldsymbol{b}_p)]\}\,.$$

As the exponential function is convex, the following relationship always holds per Jensen's inequality (Jensen (1906)):

$$S(t\,|\,t^*,\boldsymbol{w}_p,\boldsymbol{r}_p^*;\hat{\boldsymbol{\Theta}},\hat{h}_0(t)) = E\{\exp[H(\boldsymbol{b}_p)]\} \geq \exp\{E[H(\boldsymbol{b}_p)]\} = \widetilde{S}(t\,|\,t^*,\boldsymbol{w}_p,\boldsymbol{r}_p^*;\hat{\boldsymbol{\Theta}},\hat{h}_0(t))\,. \qquad (14)$$

The above inequality describes the relationship between Equation (9) and Equation (13), subject to numerical errors if approximations are used for the integrals. According to Inequality (14), the alternative estimate of the marginal survival function can be viewed as a conservative estimator rather than an approximated value: the predicted survival function yields smaller survival probability (e.g., shorter RUL prediction). For critical components and/or risk adverse users, a conservative estimator may be preferred, in addition to its computational advantage.

The proposed prognostic algorithm can update the RUL estimation as new measurements of the

degradation signal of unit p become available. For example, if an updated prediction is to be made at a time instant $t^{**} > t^{*}$ when some additional measurements have become available, an updated posterior distribution $p(\boldsymbol{b}_p \mid \boldsymbol{r}_p^{**})$ of $\boldsymbol{b}_p$ can be obtained and hence an updated estimation $\hat{S}(t \mid t^{**}, \boldsymbol{w}_p, \boldsymbol{r}_p^{**}; \hat{\boldsymbol{\Theta}}, \hat{h}_0(t))$ for the survival function. This updating process is illustrated in Figure 2.

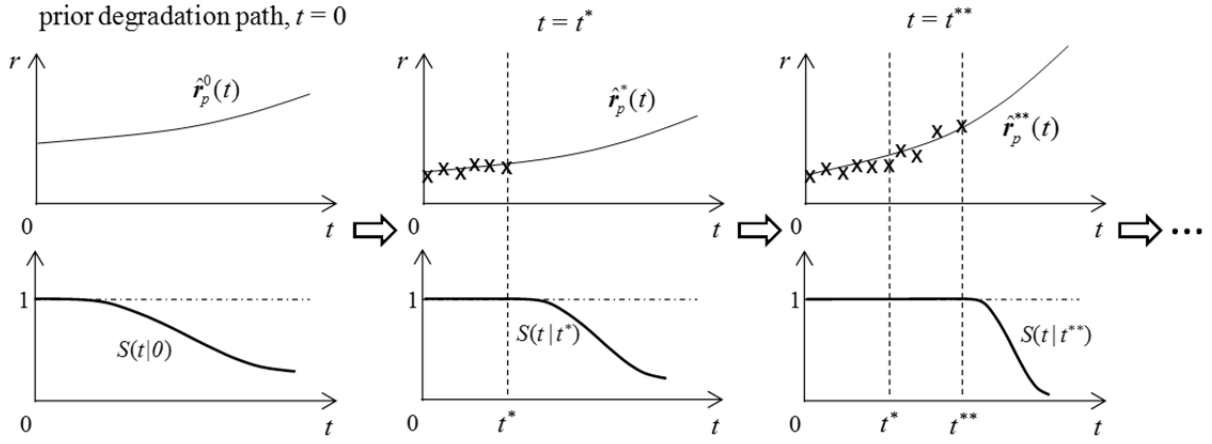

Figure 2. Updating scheme for survival function estimation

3. Simulation study

3.1. *Demonstration of the joint prognostic framework*

To demonstrate the effectiveness of the proposed algorithm, a simulation study is conducted. In the study, data are generated in the form of $D_i = \{V_i, \delta_i, \boldsymbol{r}_i^h, \boldsymbol{w}_i\}$ with N = 1000 artificial units as a database for offline stage parameter estimation. A new unit p is then generated and its RUL predicted at some time instant t^{*} during its lifetime. Estimated results are compared with the true values for assessment of prediction accuracy. Without loss of generality, in this study we assume the time unit is month, and the degradation signal measurements are obtained regularly at each month. In this simulation study, we use the Weibull baseline hazard rate function:

$$h_0(t) = \lambda\alpha t^{\alpha-1} = 0.001 \times 1.05 t^{1.05-1}.$$

We assume the underlying true degradation path has the following form

$$r_i(t) = \boldsymbol{z}^T(t)\boldsymbol{b}_i + \varepsilon_i(t) = b_{i0} + b_{i1}t^{1.2} + b_{i2}t^{1.7} + \varepsilon_i(t), \tag{15}$$

where the distribution of $\boldsymbol{b}_i$ in the simulation is set as $N(\boldsymbol{\mu}_b, \Sigma_b)$ with

$$\begin{cases} \boldsymbol{\mu}_b = [2.5, 0.01, 0.01]^T \\ \boldsymbol{\Sigma}_b = \begin{bmatrix} 0.2 & -4e-4 & 7e-5 \\ -4e-4 & 3e-6 & 1e-7 \\ 7e-5 & 1e-7 & 3e-6 \end{bmatrix} \end{cases}, \tag{16}$$

and $\sigma^2 = 0.01$. Figure 3 shows 10 randomly generated degradation signal paths based on the above path.

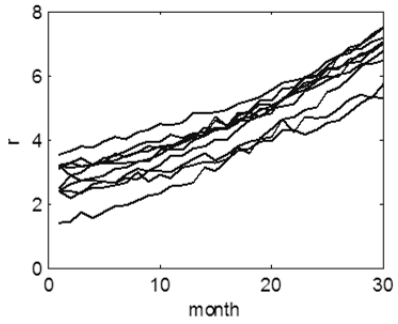

Figure 3. Example of randomly generated degradation paths

We further assume there is a time-fixed covariate w for each unit. w is a dummy variable with $w = 1$ indicating the unit is of type A and $w = 0$ indicating it is of type B. We set the associated coefficients as $\gamma = 0.20$, $\beta_0 = 0.15$, and $\beta_1 = 0.50$. Thus, the true hazard rate function of the ith unit that is used for data generation is

$$h_i(t) = 0.00105t^{0.05} \exp[0.20w_i + 0.15b_{i0} + 0.5(b_{i1}t^{1.2} + b_{i2}t^{1.7})]. \tag{17}$$

The percentage of units that are censored is set to 5%. Degradation signal of the new unit p follows the same path defined in Equation (15) with $\boldsymbol{b}_p = [3.0, 0.015, 0.012]$ and we set $w_p = 1$.

In practice, the true form of the degradation signal is rarely known; some form of growth path needs to be assumed or selected from several candidate models based on the data collected. Hence in this example, it is assumed that the true form described in Equation (15) is unknown to the algorithm and we choose a quadratic growth model to fit the data due to its simplicity and resemblance to the true curves. This intentional misspecification also helps us to examine the robustness of the proposed method under mild misspecification.

The simulation procedure is then conducted following the steps below:

Step 1: Generate realizations of $\boldsymbol{b}_i$ for each of the N = 1000 units according to (16).

Step 2: Generate failure time T_i for each unit by drawing a random sample from its probability density function $f_i(t) = h_i(t)S_i(t)$, with $h_i(t)$ defined in Equation (17). Then 5% of the units are randomly selected and censored using a uniform distribution.

Step 4: Degradation signals of each unit are generated with measurement error for every month until its time of failure or censoring.

Step 5: Model parameters (under the assumed quadratic growth model) are estimated based on the data generated above through the method described in Section 2.3.

Step 6: Degradation signal of unit p is generated based on Equation (15) and coefficient $\boldsymbol{b}_p$ with measurement error for every month until the time instant of prediction t^*.

Step 7: The RUL distribution of unit p is predicted through the two methods described in Section 2.4 with a quadratic growth, and then compared with its true value.

Step 8: Finally, Steps 1~7 are repeated for N_{rep} = 1000 times to assess the standard errors of the estimated results.

As we discussed before, the two-stage estimation method is used. First, the degradation signals are modeled through random effects model and estimates of $\{\boldsymbol{\mu}_b, \boldsymbol{\Sigma}_b, \sigma^2\}$ are obtained. Then, based on the estimated parameters, modeled values of degradation signals at any given time are provided to the survival model so that $\boldsymbol{\gamma}$, β_0, β_1, and $h_0(t)$ can be estimated.

In the RUL prediction of unit p, we have investigated its mean RUL defined as

$$mrl(t^*) = E(T - t^* \mid t^*) = \int_{t^*}^{\infty} S(u \mid t^*)du \ , \tag{18}$$

and the probabilities of failure within the next one and two years at prediction instants t^* = 0, 12, 24, 36 months. The results are given in Table 1 and Figure 4. In the table, true and estimated values of mean RUL are obtained by plugging the true and estimated survival functions into (18), respectively.

Table 1(a). Comparisons between predicted results based on Equation (12) and true values

	mrl			Pr(die within 1 year)			Pr(die within 2 years)		
	True	Estimated values		True	Estimated values		True	Estimated values	
	values	mean	std error	values	mean	std error	values	mean	std error
$t^*=0$	37.376	28.465	1.318	0.033	0.041	0.009	0.113	0.214	0.027
$t^*=12$	26.274	24.862	1.583	0.083	0.088	0.011	0.354	0.391	0.048
$t^*=24$	15.138	14.822	0.417	0.296	0.315	0.027	0.914	0.935	0.023
$t^*=36$	6.837	6.131	0.391	0.877	0.920	0.021	1.000	1.000	0.000

Table 1(b). Comparisons between predicted results based on Equation (13) and true values

	mrl			Pr(die within 1 year)			Pr(die within 2 years)		
	True	Estimated values		True	Estimated values		True	Estimated values	
	values	mean	std error	values	mean	std error	values	mean	std error
$t^*=0$	37.376	38.601	0.451	0.033	0.031	0.006	0.113	0.098	0.011
$t^*=12$	26.274	27.693	1.511	0.083	0.077	0.009	0.354	0.316	0.039
$t^*=24$	15.138	14.669	0.386	0.296	0.323	0.027	0.914	0.954	0.018
$t^*=36$	6.837	5.980	0.365	0.877	0.929	0.019	1.000	1.000	0.000

Based on the results shown in Table 1(a), 1(b) and Figure 4, the two estimating methods for the conditional survival function both provide satisfactory prediction results that are close to their corresponding true values in this example, even under the model misspecification. Generally, their prediction accuracy becomes higher as t^* increases because of the increasingly accurate estimation of degradation path as more measurements become available. This characteristic is desirable in practice as people are generally more concerned about the failure of a unit when it has been used for some time, not for a newly installed unit. Hence a crude estimate during early life time of a unit is not critical. As a special case, $t^* = 0$ indicates the predictions are made for a newly installed unit whose degradation signal is not available yet. Therefore, prediction results at $t^*= 0$ reflect population behaviors (adjusted for $w_p = 1$) of the 1000 units in the database. However, these crude initial prediction results should not deviate too much from true values of the unit p unless the new unit exhibits a drastically different behavior from those in the database.

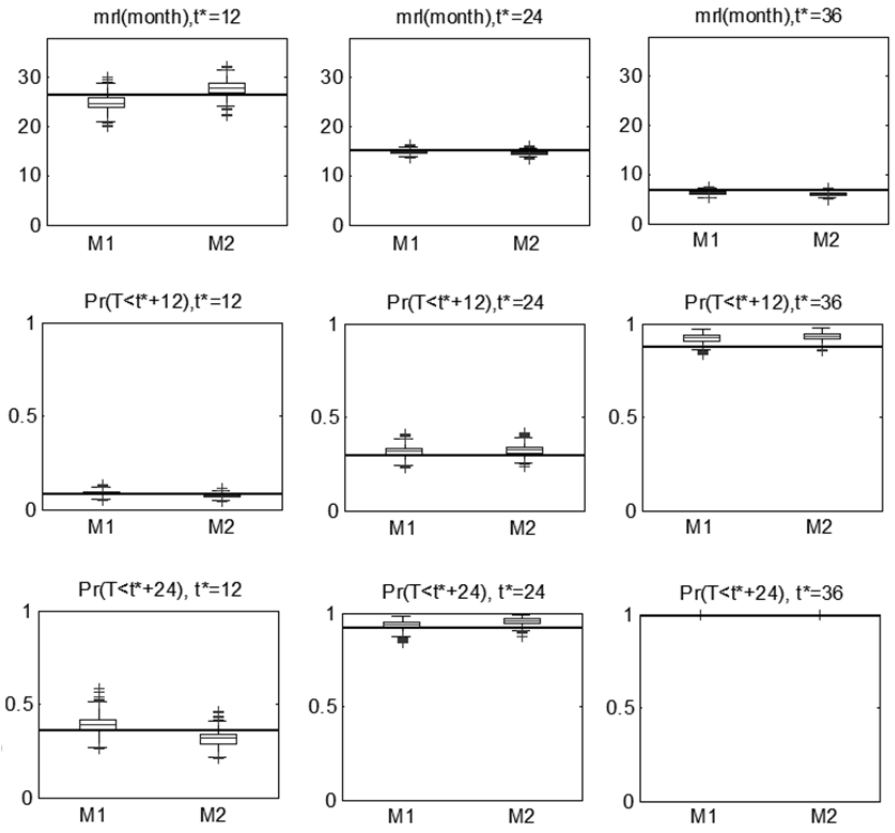

Figure 4. Boxplots for prediction results

(solid lines are true values, M1/2 indicates method based on Equation (12)/(13))

A close observation indicates that part of the results in Table 1(a) and (b) do not satisfy the relationship in (14). The mean RUL estimates presented in Table 1(a) is from Equation (12), an approximation of Equation (9) by using the Gauss-Hermite quadrature. In the Gauss-Hermite quadrature, The evaluation of $G(z)$ depends on $\hat{\boldsymbol{\mu}}_p^*$ and $\hat{\boldsymbol{\Sigma}}_p^*$, parameters with inevitable estimation errors. When those parameter estimates are not accurate enough at the early stages, the inequality may not hold. However, as the parameter estimates get more accurate, the relationship defined in the inequality holds (in this case, after $t^* = 24$).

To get a better idea of the overall performance of the proposed method, Figure 5 shows the comparison between the true conditional survival curves of unit p (in bold lines) and pointwise percentiles of the estimated curves (with median in solid lines and 2.5th/97.5th percentile in dashed lines), based on 1000

Monte Carlo samples.

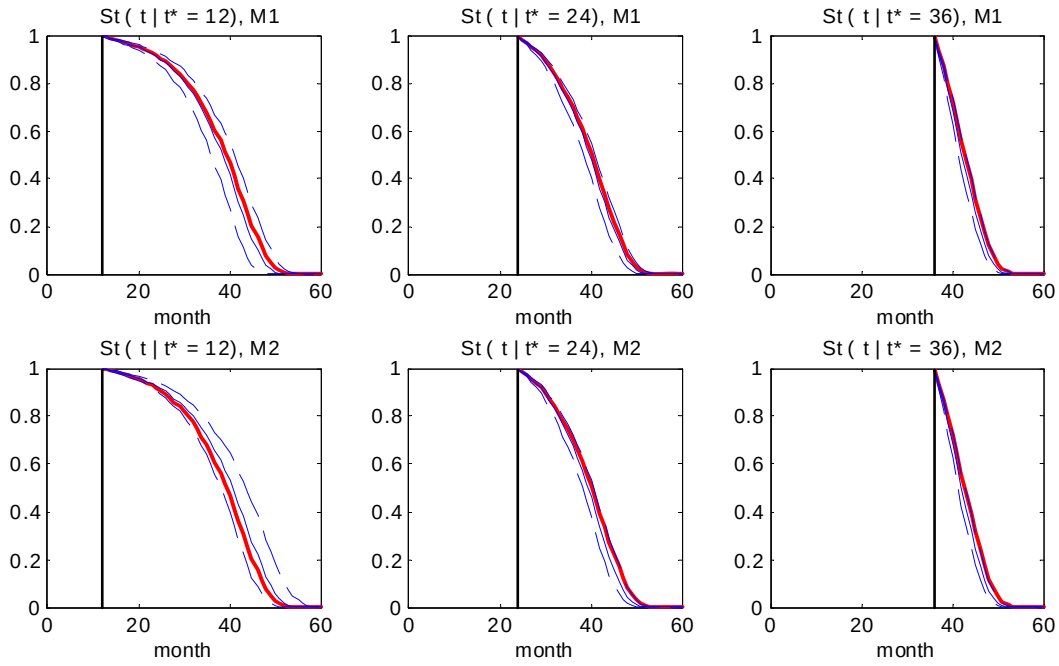

Figure 5. Comparison between true and estimated conditional survival curves at t^* = 12, 24, 36 months (bold lines: true values; solid lines: pointwise median; dashed lines: pointwise 2.5th/97.5th percentile; M1/2 indicates method based on Equation (12)/(13))

From Figure 5, we have the following observations:

(*i*) The predicted survival curves are closer to their true values when t is smaller, i.e., prediction is better for near future. This is due to the fact that the deviation between the true and projected degradation paths increases as t becomes larger.

(*ii*) The predicted survival curves are closer to their true values as t^* increases. This is due to the fact that more measurements are available (hence a more accurate model for degradation path) as t^* increases.

(*iii*) As t^* increases, the confidence interval becomes significantly narrower due to the increased amount of information about the new unit p.

In addition to the survival function discussed above, the prediction result can also be presented in the form of the failure time distribution $f(t|t^*)$. Although $S(t|t^*)$ contains the same information as $f(t|t^*)$ via the simple relationship $f(t|t^*) = -S'(t|t^*)$, it may be more convenient to examine $f(t|t^*)$ in some applications since it shows the direct distributional behavior of the failure time. The shape of $f(t|t^*)$ may also offer aid

to the decision making of maintenance strategies. The true and estimated survival functions from Equation (12) and Equation (13) in Figure 5 are converted into $f(t|t^*)$ and shown in Figure 6. Note that the pointwise intervals in Figure 5 are converted into mean curves.

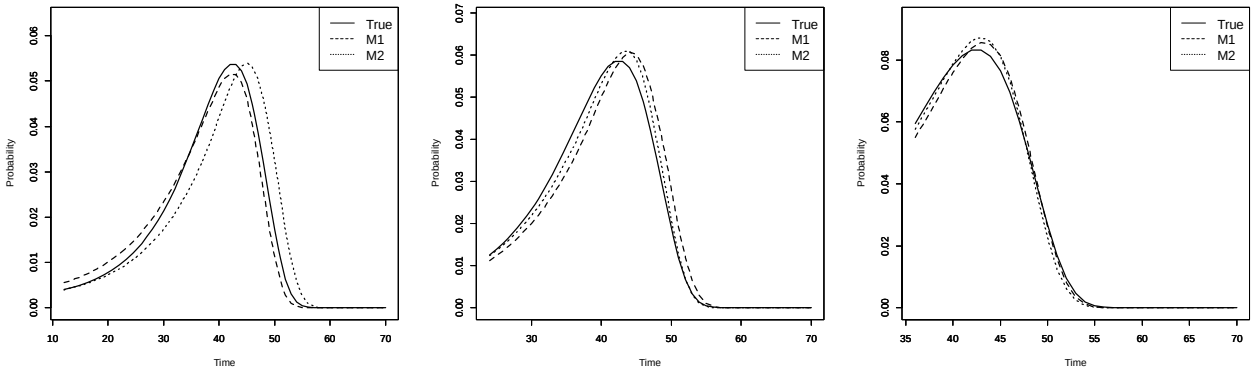

$t^* = 12$ $t^* = 24$ $t^* = 36$

Figure 6. Failure time distribution at different prediction time instants

3.2. *Performance analysis*

The simulation study conducted above is a demonstration based on a single unit with $\boldsymbol{b}_p$ = [3.0, 0.015, 0.012]. To get a better idea of the overall performance of the proposed model, more analysis has been conducted in this section.

First of all, we shall extend the simulation study to multiple units. Here, the same simulation setting from the previous section with database sample size N = 1,000 is used. The prediction performance is assessed through 3,000 in-service units with $\boldsymbol{b}_p$ values randomly sampled from the population distribution $N(\boldsymbol{\mu}_b, \boldsymbol{\Sigma}_b)$. For the performance metric, the mean absolute error (*MAE*) and the mean absolute percentage error (*MAPE*) are used. The *MAPE* is a scale-independent percentage-based measure of accuracy. Mathematical definitions for both metrics are given as

$$MAE = \frac{1}{J}\sum_{j=1}^{J}\left|mrl_j(t^*) - T_j\right|, \quad MAPE = \frac{1}{J}\sum_{j=1}^{J}\left|100\frac{mrl_j(t^*) - T_j}{T_j}\right|,$$

where $mrl_j(t^*)$ and T_j represent the mean RUL prediction at t^* and its true value for the jth unit, respectively. Table 2 summarizes the results, where the mean RUL predictions are based on Equation (12) and the J has been set as 3,000.

Table 2. *Prognostic performance summary for 3000 prediction trials*

	MAE	*MAPE*
$t^* = 0$	12.0743	28.4864
$t^* = 12$	1.9162	5.8417
$t^* = 24$	1.0943	4.7657
$t^* = 36$	0.9635	8.6903

According to the results given in Table 2, we can see that *MAE* consistently decreases as prediction time increases, confirming that the prediction accuracy gets better at the later stage of the prediction. For the scale-independent *MAPE*, although there is a small increment at the last stage of the prediction, the general decreasing trend still holds. This further confirms our previous observations.

In real-world engineering applications, a historical database with N = 1,000 samples is rarely practical. Here we demonstrate the model performance with smaller sample sizes. Table 3 presents the mean RUL prediction results based on various historical sample sizes. Note that the results are computed by Equation (12). The reduced sample size of the historical database does not cause notable problems for the parameter estimation, only with increased standard error which is expected. This shows the proposed method can be implemented with a small sample size, which may often be the case in practice.

Table 3. *Mean RUL prediction from various sample sizes*

	True values	MRL estimates (*N=1000*)		MRL estimates (*N=50*)		MRL estimates (*N=20*)	
		Mean	Std error	Mean	Std error	Mean	Std error
$t^* = 0$	37.376	28.465	1.318	29.949	4.983	33.921	9.447
$t^* = 12$	26.274	24.862	1.538	25.344	3.864	26.944	6.253
$t^* = 24$	15.138	14.822	0.417	15.147	1.909	16.377	4.507
$t^* = 36$	6.837	6.131	0.391	6.375	1.762	7.252	3.274

4. Case study on battery data

In this section, we use real data from an automotive lead-acid battery aging test to demonstrate the

proposed method. Because the aging process of automotive batteries is typically very slow and it takes several years for a battery to fail, the data is obtained from an accelerated aging test based on the aging cycle defined in SAE J2801 (SAE International (2013)). In this test, a battery is considered as dead when it fails to crank the engine. The dataset contains 15 batteries with two different types: 8 batteries of type A and 7 of type B. One battery of type A showed drastically different behavior from others and hence removed from this study. The resistance evolution of the remaining 14 batteries is shown in Figure 7. Note that resistance measurement is not necessarily available every week during the entire life of a battery. Due to confidentiality, the data presented in Figure 7 has been slightly modified from the original data, but this modification does not affect our study here. In the figure, the battery marked with stars is used for prediction and not included in the database during model fitting.

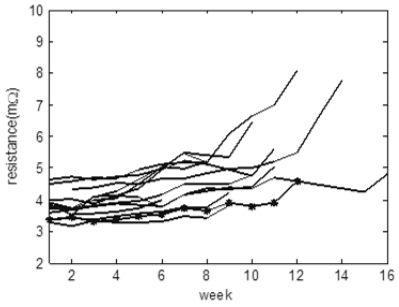

Figure 7. Battery resistance data from an accelerated aging test

(stared line: the battery to be predicted)

To the best of the authors' knowledge, there is no general physical form for the degradation path of lead-acid battery resistance. Therefore, a quadratic degradation path in the random effects model is used. Predictions are made for the battery at the $t^* = 5^{th}$ and 10^{th} week based on the resistance measurements up to these time points. With 1000 random samples generated from the posterior distribution of $\boldsymbol{b}_p$, the estimated survival curves are calculated based on Equation (8) and their point-wise quantiles shown in Figure 8.

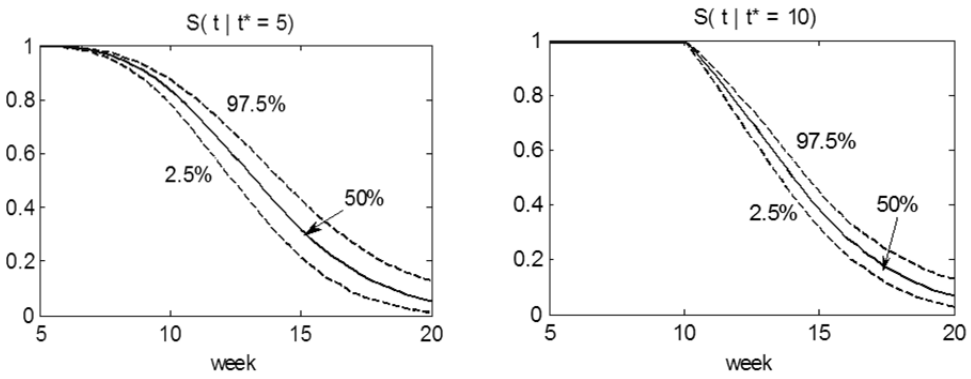

Figure 8. Estimated survival functions at t^* = 5 and 10

As expected, the point-wise interval gets narrower as more data have been collected. The estimated mean RUL of the battery is 5.99 weeks at t^* = 5 and 3.02 weeks at t^* = 10 based on Equation (12); 6.63 weeks at t^* = 5 and 2.90 weeks t^* = 10 based on Equation (13). This again shows that the prediction results are becoming more accurate at the later stage of prediction. Considering the fact that this battery actually failed at the 13th week, the prediction results are quite good.

5. Conclusions

In this paper, a prognostic framework based on the joint modeling of time-to-event data and degradation signal has been proposed for RUL prediction of individual units under hard failure. The framework features a two-stage approach where modeling and parameter estimation are done offline based on historical data of previously recorded units, and online real-time RUL prediction for new units being used in the field. This two-stage approach allows the prediction to be made quickly with minimal requirement on computation; hence it has the potential to be implemented on individual units in the field where powerful computing platforms are not available (e.g., the prediction of a battery RUL on a vehicle micro-controller). Two methods for estimating the conditional survival function have been proposed and tested in a simulation study. The Equation (12) is accurate but relatively slow, while Equation (13) is a conservative estimator but significantly faster. The choice of the two methods should be made depending on the actual application: (13) is preferred for risk adverse users and/or when computational load is of primary concern.

In this paper, assessment of the algorithm's prediction accuracy is rather subjective due to lack of rigorous methods in the related literature. In engineering applications, a preferable method for assessing predictive accuracy should be based on some commonly accepted criteria such as Type I and II error rates. Also, this study focuses on the mean RUL point estimate. In practice, the interval estimate gives richer information to the user than the point estimate. Since the RUL distribution is readily available from the proposed joint prognostic framework, constructing the failure prediction interval could be an interesting topic to investigate. These will be studied and reported in future.

Acknowledgements

This work is supported by the National Science Foundation CMMI Grant # 1335129 and the National Natural Science Foundation of China Grant # 11301441. The authors wish to thank the Associate Editor and three referees for their helpful comments that have led to improvements of this paper.

References

Bycott, P., and Taylor, J. (1998) A comparison of smoothing techniques for CD4 data measured with error in a time-dependent Cox proportional hazards model. *Statistics in Medicine*, **17**(18), 2061-2077.

Cox D.R. (1972) Regression models and life-tables. *Journal of the Royal Statistical Society*, *Series B*, **34**, 187-220.

Cugnet, M., Sabatier, J., Laruelle, S., Grugeon, S., Sahut, B., Oustaloup, A., and Tarascon, J. (2010) On lead-acid-battery resistance and cranking-capability estimation *IEEE Transactions on Industrial Electronics*, **57**(3), 909-917.

Elwany, A., and Gebraeel, N. (2009) Real-time estimation of mean remaining life using sensor-based degradation models. *Journal of Manufacturing Science and Engineering*, **131**(5), 051005-1-051005-9.

Gebraeel, N. (2006) Sensory-updated remaining useful life distributions for components with exponential degradation signals. *IEEE Transactions on Automation Science and Engineering*, **3**(4), 382-393.

Gebraeel, N., Lawley, R., Li, R., and Ryan, J. (2005) Residual-life distributions from component degradation signals: A Bayesian approach. *IIE Transactions*, **37**(6), 543-557.

Gorjian, N., Ma, L, Mittinty, M., Yarlagadda, P., and Sun, Y. (2009) A review on degradation models in reliability analysis. *Proceedings of the 4th World Congress on Engineering Asset Management*, Athens, Greece, Sep. 2009.

Hsieh, F., Tseng, Y-K., and Wang, J-L. (2006) Joint modeling of survival and longitudinal data: likelihood approach revisited. *Biometrics*, **62**(4), 1037-1043.

Jardine, A., Lin, D., and Banjevic, D. (2006) A review on machinery diagnostics and prognostics implementing condition-based maintenance. *Mechanical Systems and Signal Processing*, **20**(7), 1483-1510.

Jensen, J. L. W. V. (1906) Sur les fonctions convexes et les inégalités entre les valeurs moyennes *Acta Mathematica*. **30**(1), 175-193.

Laird, N. M., and Ware, J.H. (1982) Random effects model for longitudinal data. *Biometrics*, **38**(4), 963-973.

Liao, H., Zhao, W., and Guo, H. (2006) Predicting remaining useful life of an individual unit using proportional hazards model and logistic regression model. *Proceedings of the Annual Reliability and Maintainability Symposium*, Newport Beach, CA, 2006.

Lu, C., and Meeker, W. (1993) Using degradation measures to estimate a time-to-failure distribution. *Technometrics*, **35**(2), 161-174.

Pauler, D. K., and Finkelstein, D.M. (2002) Predicting time to prostate cancer recurrence based on joint models for non-linear longitudinal biomarkers and event time outcomes. *Statistics in Medicine*, **21**(24), 3897-3911.

Prentice, R. L. (1982) Covariate measurement errors and the parameter estimation in a failure time regression model. *Biometrika*, **69**(2), 331-342.

Rizopoulos, D. (2011) Dynamic predictions and prospective accuracy in joint models for longitudinal and time-to-event data. *Biometrics*, **67**(3), 819-829.

Rizopoulos, D., and Verbeke, G. (2008) Shared parameter models under random effects misspecification. *Biometrika*, **95**(1), 63-74.

SAE International (2013) Comprehensive Life Test for 12 V Automotive Storage Batteries. SAE Standards J2801.

Tsiatis, A., and Davidian, M. (2004) Joint modeling of longitudinal and time-to-event data: an overview. *Statistica Sinica*, **14**(3), 809-834.

Tsiatis, A., DeGruttola, V., and Wulfsohn, M.S. (1995) Modeling the Relationship of Survival to Longitudinal Data Measured with Error. Applications to Survival and CD4 Counts in Patients with AIDS. *Journal of American Statistical Association*, **90**(429), 27-37.

Wang, P., and Coit, D. (2007) Reliability and degradation modeling with random or uncertain failure threshold. *Proceedings of the Annual Reliability and Maintainability Symposium*, Las Vegas, NV, 2007.

Wang, Y., and Taylor, J. (2001) Jointly modeling longitudinal and event time data with application to acquired immunodeficiency syndrome. *Journal of American Statistical Association*, **96**(455), 895-905.

Wulfsohn, M., and Tsiatis, A. (1997) A joint model for survival and longitudinal data measured with error. *Biometrics*, **53**, 330-339.

Ye, Z.S., and Chen, N. (2014) The inverse Gaussian process as a degradation model. *Technometrics*, to appear.

Ye, Z.S., Shen, Y., and Xie, M. (2012) Degradation-based burn-in with preventive maintenance. *European Journal of Operational Research*, **221** (2), 360-367.

Yu, I.T., and Fuh, C.D. (2010) Estimation of Time to Hard Failure Distributions Using a Three-Stage Method. *IEEE Transactions on Reliability*, **59**(2), 405-412.

Yu, M., Law, N., Taylor, J., and Sandler, H. (2004) Joint longitudinal-survival-cure models and their application to prostate cancer. *Statistica Sinica*, **14**(3), 835-862.

Yu, M., Taylor, J., and Sandler, H. (2008) Individual prediction in prostate cancer studies using a joint longitudinal survival-cure model. *Journal of American Statistical Association*, **103**(481), 178-187.

Zhang, X., Grube, R., Shin, K-K, Salman, M., and Conell, R. (2011) Parity-relation-based state-of-health monitoring of lead acid batteries for automotive applications. *Control Engineering Practice*, **19**(6), 555-563.

Appendix

The likelihood function (7) can be rewritten in a matrix form as

$$p(\boldsymbol{r}_p^{h*} \mid \boldsymbol{b}_p) = (2\pi\hat{\sigma}^2)^{-m/2} \exp\left[-(\boldsymbol{r}_p^{h*} - \boldsymbol{Z}_p^* \boldsymbol{b}_p)^T (\boldsymbol{r}_p^{h*} - \boldsymbol{Z}_p^* \boldsymbol{b}_p) / (2\hat{\sigma}^2)\right].$$

Based on prior distribution $\pi(\boldsymbol{b}_p) = N(\hat{\boldsymbol{\mu}}_b, \hat{\boldsymbol{\Sigma}}_b)$, the posterior distribution of $\boldsymbol{b}_p$, is

$$
\begin{aligned}
& p(\boldsymbol{b}_p \mid \boldsymbol{r}_p^{h^*}) \propto p(\boldsymbol{r}_p^{h^*} \mid \boldsymbol{b}_p)\pi(\boldsymbol{b}_p) \\
& \propto \exp\left\{-\frac{1}{2\hat{\sigma}^2}\left[(\boldsymbol{r}_p^{h^*}-\boldsymbol{Z}_p^*\boldsymbol{b}_p)^T(\boldsymbol{r}_p^{h^*}-\boldsymbol{Z}_p^*\boldsymbol{b}_p)\right]\right\}\exp\left\{-\frac{1}{2}\left[(\boldsymbol{b}_p-\hat{\boldsymbol{\mu}}_b)^T\hat{\boldsymbol{\Sigma}}_b^{-1}(\boldsymbol{b}_p-\hat{\boldsymbol{\mu}}_b)\right]\right\} \\
& \propto \exp\left\{-\frac{1}{2\hat{\sigma}^2}\left[(\boldsymbol{r}_p^{h^*})^T\boldsymbol{r}_p^{h^*}-\boldsymbol{b}_p^T(\boldsymbol{Z}_p^*)^T\boldsymbol{r}_p^{h^*}-(\boldsymbol{r}_p^{h^*})^T\boldsymbol{Z}_p^*\boldsymbol{b}_p+\boldsymbol{b}_p^T(\boldsymbol{Z}_p^*)^T\boldsymbol{Z}_p^*\boldsymbol{b}_p\right]\right\} \\
& \quad \times\exp\left\{-\frac{1}{2}\left[\boldsymbol{b}_p^T\hat{\boldsymbol{\Sigma}}_b^{-1}\boldsymbol{b}_p-\hat{\boldsymbol{\mu}}_b^T\hat{\boldsymbol{\Sigma}}_b^{-1}\boldsymbol{b}_p-\boldsymbol{b}_p^T\hat{\boldsymbol{\Sigma}}_b^{-1}\hat{\boldsymbol{\mu}}_b+\hat{\boldsymbol{\mu}}_b^T\hat{\boldsymbol{\Sigma}}_b^{-1}\hat{\boldsymbol{\mu}}_b\right]\right\} \\
& \propto \exp\left\{-\frac{1}{2}\left[\boldsymbol{b}_p^T\left(\frac{(\boldsymbol{Z}_p^*)^T\boldsymbol{Z}_p^*}{\hat{\sigma}^2}+\hat{\boldsymbol{\Sigma}}_b^{-1}\right)\boldsymbol{b}_p-\boldsymbol{b}_p^T\left(\frac{(\boldsymbol{Z}_p^*)^T\boldsymbol{r}_p^{h^*}}{\hat{\sigma}^2}+\hat{\boldsymbol{\Sigma}}_b^{-1}\hat{\boldsymbol{\mu}}_p\right)-\left(\frac{(\boldsymbol{r}_p^{h^*})^T\boldsymbol{Z}_p^*}{\hat{\sigma}^2}+\hat{\boldsymbol{\mu}}_b^T\hat{\boldsymbol{\Sigma}}_b^{-1}\right)\boldsymbol{b}_p+C_1\right]\right\} \\
& \propto \exp\left\{-\frac{1}{2}\left[\boldsymbol{v}^T\left(\frac{(\boldsymbol{Z}_p^*)^T\boldsymbol{Z}_p^*}{\hat{\sigma}^2}+\hat{\boldsymbol{\Sigma}}_b^{-1}\right)\boldsymbol{v}+C_2\right]\right\}
\end{aligned}
\qquad ,(A1)
$$

where C_1 and C_2 are constants not involving $\boldsymbol{b}_p$, and $\boldsymbol{v}$ is a $k\times 1$ vector defined as

$$
\boldsymbol{v}=\boldsymbol{b}_p-\left(\frac{(\boldsymbol{Z}_p^*)^T\boldsymbol{Z}_p^*}{\hat{\sigma}^2}+\hat{\boldsymbol{\Sigma}}_b^{-1}\right)^{-1}\left(\frac{(\boldsymbol{Z}_p^*)^T\boldsymbol{r}_p^{h^*}}{\hat{\sigma}^2}+\hat{\boldsymbol{\Sigma}}_b^{-1}\hat{\boldsymbol{\mu}}_b\right).
$$

Define

$$
\begin{cases}
\hat{\boldsymbol{\mu}}_p^*=\left(\dfrac{(\boldsymbol{Z}_p^*)^T\boldsymbol{Z}_p^*}{\hat{\sigma}^2}+\hat{\boldsymbol{\Sigma}}_b^{-1}\right)^{-1}\left(\dfrac{(\boldsymbol{Z}_p^*)^T\boldsymbol{r}_p^{h^*}}{\hat{\sigma}^2}+\hat{\boldsymbol{\Sigma}}_b^{-1}\hat{\boldsymbol{\mu}}_b\right), \\
\hat{\boldsymbol{\Sigma}}_p^*=\left(\dfrac{(\boldsymbol{Z}_p^*)^T\boldsymbol{Z}_p^*}{\hat{\sigma}^2}+\hat{\boldsymbol{\Sigma}}_b^{-1}\right)^{-1}
\end{cases}
$$

the result in (A1) can be rewritten as

$$
p(\boldsymbol{b}_p \mid \boldsymbol{r}_p^{h^*}) \propto \left\{-\frac{1}{2}\left[\left(\boldsymbol{b}_p-\hat{\boldsymbol{\mu}}_p^*\right)^T\left(\hat{\boldsymbol{\Sigma}}_p^*\right)^{-1}\left(\boldsymbol{b}_p-\hat{\boldsymbol{\mu}}_p^*\right)\right]\right\}.
$$

The above density defines a k-dimensional multivariate normal distribution $N(\hat{\boldsymbol{\mu}}_p^*,\hat{\boldsymbol{\Sigma}}_p^*)$. □